

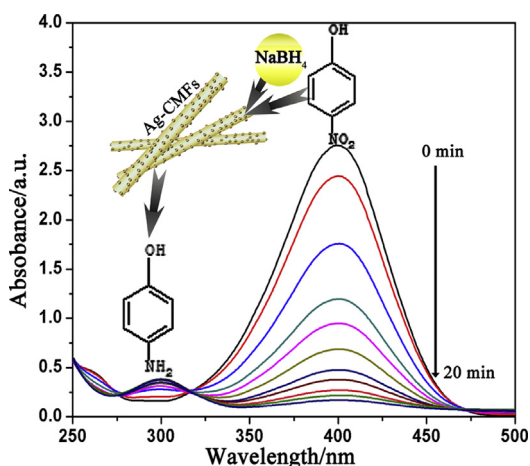
## Regular Article

## Facile fabrication of silver nanoparticles deposited cellulose microfiber nanocomposites for catalytic application

Peng Xu<sup>a</sup>, Changli Cen<sup>a</sup>, Nannan Chen<sup>a</sup>, Huan Lin<sup>a</sup>, Qing Wang<sup>a</sup>, Nanfang Xu<sup>b</sup>, Jingen Tang<sup>b</sup>, Zhaogang Teng<sup>c,\*</sup><sup>a</sup> College of Chemical Engineering, Nanjing Forestry University, Nanjing 210037, China<sup>b</sup> College of Forestry, Nanjing Forestry University, Nanjing 210037, China<sup>c</sup> Department of Medical Imaging, Jinling Hospital, School of Medicine, Nanjing University, Nanjing 210002, China

## GRAPHICAL ABSTRACT

Silver nanoparticles deposited cellulose microfibers (Ag-CMFs) were successfully prepared, which exhibit excellent catalytic performance for the reduction of *p*-nitrophenol to *p*-aminophenol in the presence of NaBH<sub>4</sub> at room temperature in aqueous media.



## ARTICLE INFO

## Article history:

Received 4 February 2018

Revised 9 April 2018

Accepted 9 April 2018

Available online 11 April 2018

## Keywords:

Silver  
Cellulose  
Microfiber  
Electrospinning  
Catalysis

## ABSTRACT

In this study, we have prepared silver nanoparticles deposited cellulose microfibers (Ag-CMFs) with excellent catalytic property. The cellulose microfibers with a mean diameter of approximately 270 nm are regenerated by deacetylation of cellulose acetate microfibers. Silver nanoparticles are deposited onto the surface of the cellulose microfibers by a simple wet reduction of silver precursor using glucose as reducing agent. The morphology, thermal stability and catalytic activities of the samples have been investigated by scanning electron microscopy (SEM), transmission electron microscopy (TEM), energy dispersive spectroscopy (EDS), X-ray diffraction (XRD), Fourier transform infrared spectroscopy (FTIR), thermogravimetric analysis (TG), and UV–vis spectrophotometer. The average size of Ag nanoparticles deposited on the fibers is approximately  $10 \pm 5$  nm, and the deposition of the Ag nanoparticles does not change the morphology of the cellulose microfibers. The obtained Ag-CMFs exhibit excellent catalytic

\* Corresponding author.

E-mail address: [zhaogangteng@163.com](mailto:zhaogangteng@163.com) (Z. Teng).

activity and reusable character for the reduction of *p*-nitrophenol by sodium borohydride. Therefore, the Ag-CMFs prepared by the facile method is expected to be an effective and promising catalytic material.  
© 2018 Elsevier Inc. All rights reserved.

## 1. Introduction

In recent years, electrospinning has been acknowledged as one of the most versatile and effective techniques to fabricate continuous microfibers with controllable morphologies, structures, and functional components. Different kinds of electrospun fibrous membranes such as polypyrrolidone [1], poly(vinyl alcohol) [2], polyurethane [3], silica, and titanium [4–6] have been developed for applications in filtration [7,8], biomedicine [9,10], catalysis [11–13], and sensors [14]. Nevertheless, most of the electrospun fibers are undegradable and expensive [15]. Hence, developing efficient, green and easily handleable electrospun microfibers becomes an important task.

Cellulose, as the most abundant and renewable bioresource, is widely used as one of the most promising raw materials for the fabrication of various high performance functional materials [16]. Electrospun nanofibers of cellulose and their derivatives have been successfully fabricated and widely used as the supports for the active metal nanoparticles. Cellulose acetate (CA) nanofibers containing AgNPs have been prepared by reducing Ag<sup>+</sup> ions on CA nanofibers by electrospun from a CA solution with AgNO<sub>3</sub> [17]. The AgNPs were stabilized by the interaction with the carbonyl oxygen groups in the CA and exhibited very strong antimicrobial activity [18,19]. In addition, AgNPs adsorbed on the carboxylic ion functionalized cellulose nanofibers for catalytic activity has also been reported by Mayakrishnan Gopiraman and co-workers [20,21]. Compared with fibers of cellulose derivatives, cellulose fibers have better hydrophilicity and more stable mechanical properties for contacting with nanoparticles and organic pollutants [22]. Moreover, the rich hydroxyl groups on the surface of the cellulose fibers can easily assist the formation of fine nanoparticles with good dispersion and adhesion. Hence, cellulose fibers have the potential to be utilized as supporting materials for the preparation of form-stable metal nanocomposites especially for catalytic applications.

In this work, silver nanoparticles deposited cellulose microfibers (Ag-CMFs) were synthesized by a simple and efficient method via deacetylation of the electrospun cellulose acetate microfibers into cellulose microfibers, and then the AgNPs were deposited onto the surface of cellulose microfibers by a wet synthesis method. The cellulose microfibers exhibited improved hydrophilicity after deacetylation. AgNPs with a size of 10 ± 5 nm are uniformly dispersed on the surface of the cellulose microfibers. The catalytic performance and repeatability of Ag-CMFs nanocomposites for the reduction of *p*-nitrophenol (4-NP) to *p*-aminophenol (4-AP) were evaluated in the presence of NaBH<sub>4</sub>.

## 2. Experimental section

### 2.1. Materials and methods

Cellulose acetate (CA, 54.5–56% acetyl content), sodium borohydride (NaBH<sub>4</sub>, AR), *p*-nitrophenol (4-NP), and glucose were purchased from Sinopharm Chemical Reagent Co. Ltd.(China). Acetone, *N,N*-dimethylformamide (DMF), silver nitrate (AgNO<sub>3</sub>, ≥99.8%), ammonia sodium, sodium hydroxide (NaOH), potassium hydroxide (KOH), and sodium borohydride (NaBH<sub>4</sub>, 98%) were obtained from Nanjing Chemical Reagent Co. Ltd. (China). All chemicals were used as received and without further purification.

### 2.2. Fabrication of cellulose microfibers (CMFs)

Cellulose acetate (CA) was dissolved in mixture of acetone/DMF with a volume ratio of 3:2 and stirred at 60 °C for 4 h to obtain the homogeneous solution which is used as a precursor solution for electrospinning. In the process, CA solution was pumped into a stainless needle tip with an orifice diameter of 0.67 mm from a syringe system (CTN-TCI-V). The CA solution was ejected from the stainless steel needle with a voltage(DW-p303-1ACF0) of 20 kV at an ejected rate of 0.5 mL/h. The distance between the needle and the collector was maintained at 15 cm. The electrospun fibrous mats were collected on tin foil papers and then dried overnight at ambient temperature to remove the residue solvent. Then electrospun CA microfibers were separated from the tin foil sheet collector and deacetylated in 0.5 M KOH alcohol solution to hydrolysis into cellulose for 3 h. Then the cellulose microfibrillar mats were then rinsed with distilled water to neutralize the pH and dried at ambient temperature.

### 2.3. Synthesis of silver nanoparticles deposited cellulose microfibers (Ag-CMFs)

The preparation procedure of AgNPs deposited cellulose microfibers includes the coating of the cellulose microfibers with silver ions, followed by a facile reduction procedure by glucose. Specifically, 50 mg of the as-prepared CMFs was immersed into the fresh silver ammonia solution (0.05 M), then 1 mL of glucose solution (0.12 M) was added dropwise to the above solution at room temperature for 3 h. The sample was taken out, washed with water, and freeze-dried for 48 h.

### 2.4. Characterization

Scanning electron microscope (SEM) images were obtained on a JSM-7600F electron microscope (Rigaku, Japan). The average diameter of cellulose-based microfibers was determined from the SEM image using ImageJ software (National Institutes of Health, MD, USA). The chemical compositions of the Ag-CMFs were investigated using an energy dispersive spectrometer (EDS) attached to the JSM-7600F SEM. Transmission electron microscopy (TEM) images were obtained on a JEM1400 electron microscope (Rigaku, Japan). The catalytic reduction was monitored by an UV-2450 UV-vis (SHIMADZU, Japan) spectroscope. X-ray diffraction (XRD) patterns were obtained on an Ultima IV (Rigaku, Japan) and the scanning was running from 30° to 80° at the speed of 5°/min. The FTIR spectra of all samples were recorded on an attenuated total reflection Fourier transform infrared instrument (Nicolet, PerkinElmer, USA) with smart iTR module in the range of 4000–400 cm<sup>-1</sup> with a resolution of 4 cm<sup>-1</sup>. The static water contact angles on the cellulose acetate microfibers and cellulose microfibers were evaluated using a contact angle analyzing instrument (JC2000D1, POWEREACH, China) at room temperature. Thermal properties of the samples were investigated by thermal analyzer (Q5000IR, TA, USA) at temperature range of 20 °C–700 °C with a heating rate of 10 °C/min and nitrogen gas flow rate of 10 mL/min.

### 2.5. Catalytic reduction of 4-NP

The reduction of 4-NP by the Ag-CMFs nanocomposites in the presence of an excess amount of NaBH<sub>4</sub> was studied and monitored

by a UV–vis spectroscopy to examine the catalytic activity at room temperature. The reaction procedure was as follows: 6 mL of 2 mmol/L 4-NP was added to 2 mL of 0.5 mol/L NaBH<sub>4</sub> aqueous solution, and the solution color turned to bright yellow rapidly. Subsequently, particular amount of catalysts were added and stirred. After the addition of Ag-CMFs, the characteristic absorption peak of 4-nitrophenolate ion at 400 nm gradually decreased. Simultaneously, a new peak at 300 nm, ascribable to the newly generated 4-AP, emerged [23]. The absorption spectra of the solution were recorded in the range of 250–550 nm.

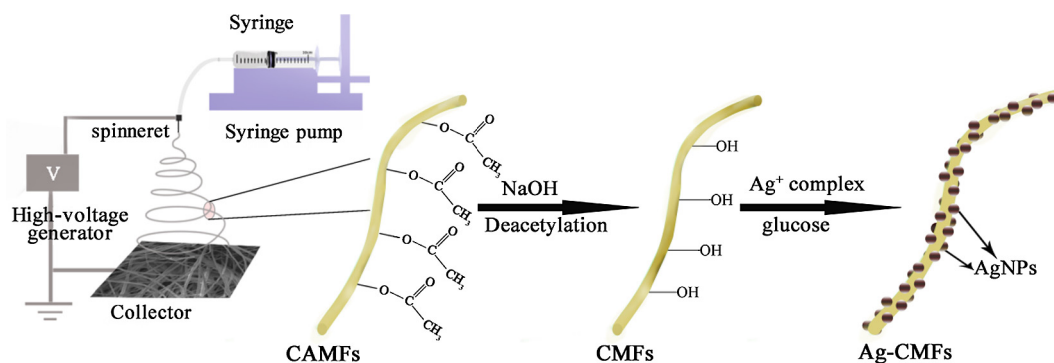
In order to investigate the reusability of the as-synthesized catalyst, the used Ag-CMFs nanocomposites were separated from the reaction solution and washed three times with distilled water and subsequently subjected to the next reaction without any drying treatment.

### 3. Results and discussion

The preparation procedure of Ag-CMFs nanocomposite based on the electrospinning method is illustrated in Scheme 1. Cellulose

acetate microfibrils (CAMFs) were electrospun followed by deacetylation to produce cellulose microfibrils (CMFs). After mixing the CMFs with silver ammonia solution, the hydroxyl groups presenting on the surface of cellulose microfibrils act as strong anchoring sites to immobilize Ag ions. Finally, the immobilized Ag ions on the CMFs are reduced by glucose to uniform Ag nanoparticles to form the Ag-CMFs.

SEM images of the CAMFs and CMFs show smooth and regular morphologies (Fig. 1), and there are no obvious changes except for the diameter of the microfibrils during the deacetylation with NaOH. The diameters of the microfibrils are measured to be approximately 400 nm and 270 nm for CAMFs and CMFs, respectively (Fig. 1c and d). The hydrophilic property of the microfibrils is characterized by the contact angle. The water droplet quickly spread and wetted the cellulose microfibrils compared to cellulose acetate microfibrils (Insets in Fig. 1a and b). The contact angles for CAMFs and CMFs are 124.8 °C and 9.85 °C, respectively, which indicates that the hydrophilic property of microfibrils has been greatly improved by the process of deacetylation.



Scheme 1. The synthesis process of the Ag-CMFs.

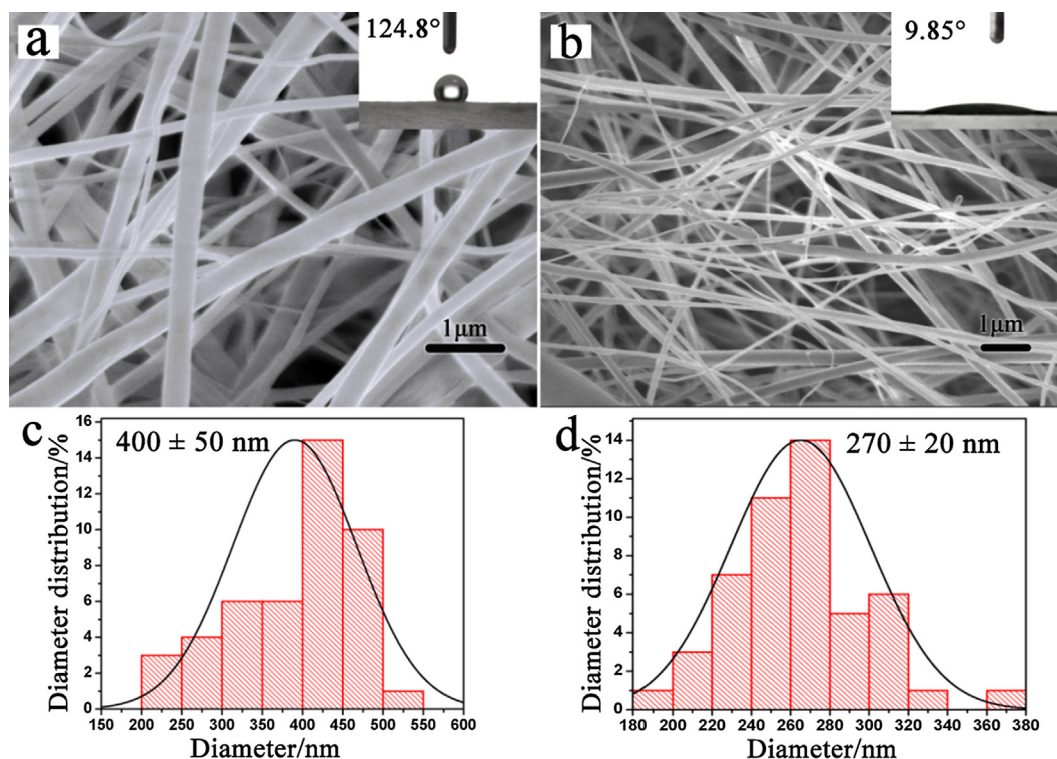


Fig. 1. SEM images and contact angles of the CAMFs (a) and CMFs (b). The diameter distribution of CAMFs (c) and CMFs (d).

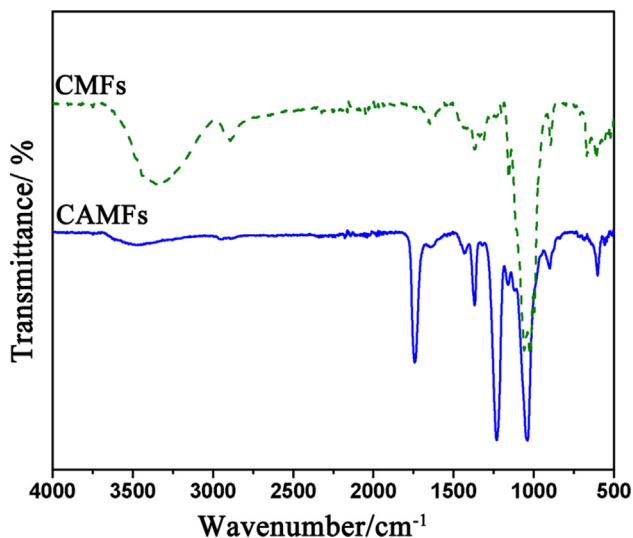


Fig. 2. FTIR spectra of CAMFs and CMFs.

The FTIR method was employed to analyze the CAMFs and CMFs (Fig. 2). The spectra of CAMFs show three intense peaks at  $1742\text{ cm}^{-1}$ ,  $1373\text{ cm}^{-1}$ , and  $1235\text{ cm}^{-1}$  corresponding to the stretching vibrations of C=O, C–CH<sub>3</sub> and C–O–C groups, respectively [24]. After deacetylation, the signal of C=O disappears and a strong hydroxyl (–OH) absorption peak at  $3376\text{ cm}^{-1}$  arises, indicating the successful conversion of cellulose acetate to cellulose [25].

SEM morphology observation shows the AgNPs have been well deposited on the surface of the cellulose microfibrils (Fig. 3a). As revealed by transmission electron microscopy (TEM), Fig. 3b shows that AgNPs with a diameter of  $10 \pm 5\text{ nm}$  are uniformly dispersed on the surface of CMFs. The successful deposition of AgNPs is also supported by the EDS analysis (Fig. 3c), and the mass fraction of Ag, C and O was measured to be 30.8 wt%, 51.3 wt%, and 17.6 wt%, respectively. The XRD patterns of CMFs and Ag-CMFs are shown in Fig. 3f. CMFs exhibit a smooth curve with no obvious diffraction peak. For Ag-CMFs, four diffraction peaks at  $2\theta$  angles of  $38.0^\circ$ ,  $44.2^\circ$ ,  $64.4^\circ$  and  $77.2^\circ$  are observed, corresponding to the (1 1 1), (2 0 0), (2 2 0), and (3 1 1) crystalline plane, suggesting the face-centered cubic of silver. The results demonstrate that AgNPs with good crystallinity have been successfully deposited onto the CMFs.

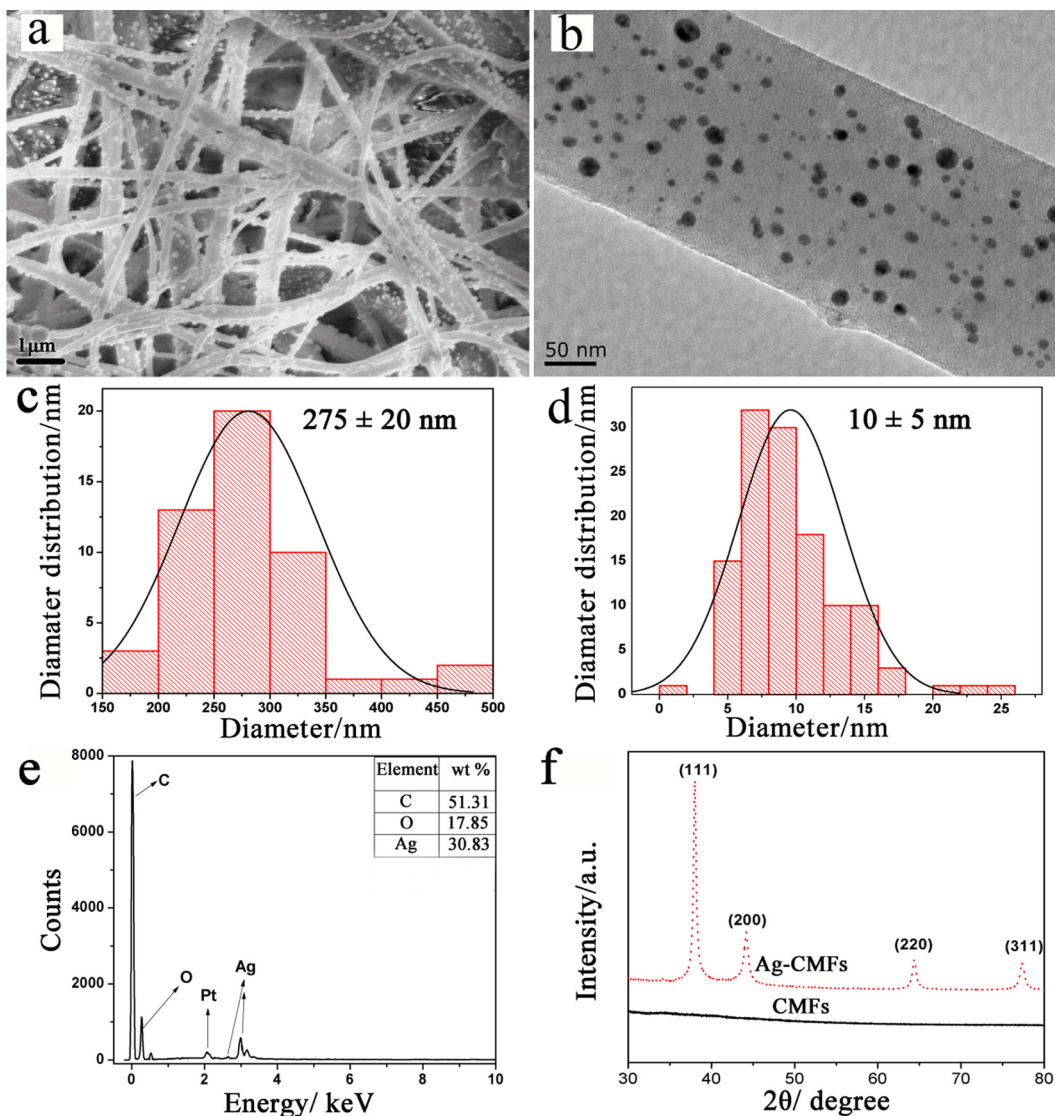


Fig. 3. SEM micrograph of Ag-CMFs nanocomposites (a). TEM image of the Ag-CMFs nanocomposites (b). (c) and (d) are the diameter distributions of the microfibrils and Ag nanoparticles, respectively. EDS spectra and atomic ratio of corresponding elements in the Ag-CMFs composites (e). XRD patterns of the Ag-CMFs and CMFs (f).

Thermal stability of CMFs and Ag-CMFs was evaluated by TG. For CMFs, there are mainly two weight-loss stages below 100 °C and 300–400 °C (Fig. 4), in which the first weight-loss stage corresponds to the evaporation of physically adsorbed water and the second weight loss of about 85% is due to the decomposition and carbonization of cellulose. The TG curve of Ag-CMFs shows a total loss of about 65% with the same initial decomposition as CMFs. Obviously, the deposition of AgNPs did not change the thermal stability of the CMFs.

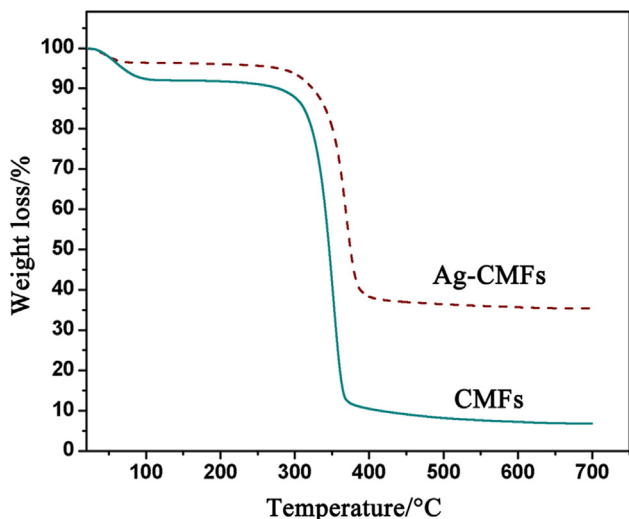


Fig. 4. TG graphs of the CMFs and Ag-CMFs.

The reduction of *p*-nitrophenol (4-NP) by excess  $\text{NaBH}_4$  was chosen as a model reaction to investigate the catalytic activity of the prepared samples. Generally, the investigation was carried out under ambient conditions. The 4-NP solution shows a strong absorption peak at 317 nm in neutral, upon the addition of freshly prepared  $\text{NaBH}_4$  solution, the position of the characteristic absorption shifts to 400 nm with a color change from light yellow to yellow-green, indicating the formation of 4-nitrophenolate ions in alkaline condition (Fig. 5a). Despite that  $\text{NaBH}_4$  is a strong reducing agent, the absorption peak at 400 nm and the intensity of the characteristic peak for 4-NP were unchanged after a long time incubation [26,27]. The catalytic ability of the CMFs was examined by adding them into the mixture of 4-NP and  $\text{NaBH}_4$  solution, as seen in Fig. 5b, there is little influence on the change in absorbance at 400 and 300 nm, indicating that under the experimental condition, the reduction of 4-NP does not proceed in the presence of CMFs.

Fig. 5c unambiguously exhibits the time-dependent UV-vis absorption spectra changed for a typical reduction process using Ag-CMFs as the catalysts. The intensity of the absorption peak at 400 nm decreased with increasing reaction time, and the intensity of the *p*-aminophenol (4-AP) absorption at 300 nm correspondingly increased, 4-NP was almost reduced after reaction for 20 min. As the concentration of  $\text{NaBH}_4$  largely exceeds the concentration of 4-NP, it can be considered as a constant during the reaction period. Since the absorbance of 4-NP is proportional to its concentration in the medium, the ratio of absorbance at time  $t$  ( $A_t$ ) to that at  $t = 0$  ( $A_0$ ) must be equal to the concentration ratio  $C_t/C_0$  of 4-NP. Consequently, the conversion progress could be directly reflected by the absorption intensity. Thus, the pseudo-first-order kinetics with regard to the 4-NP concentration can be used to evaluate

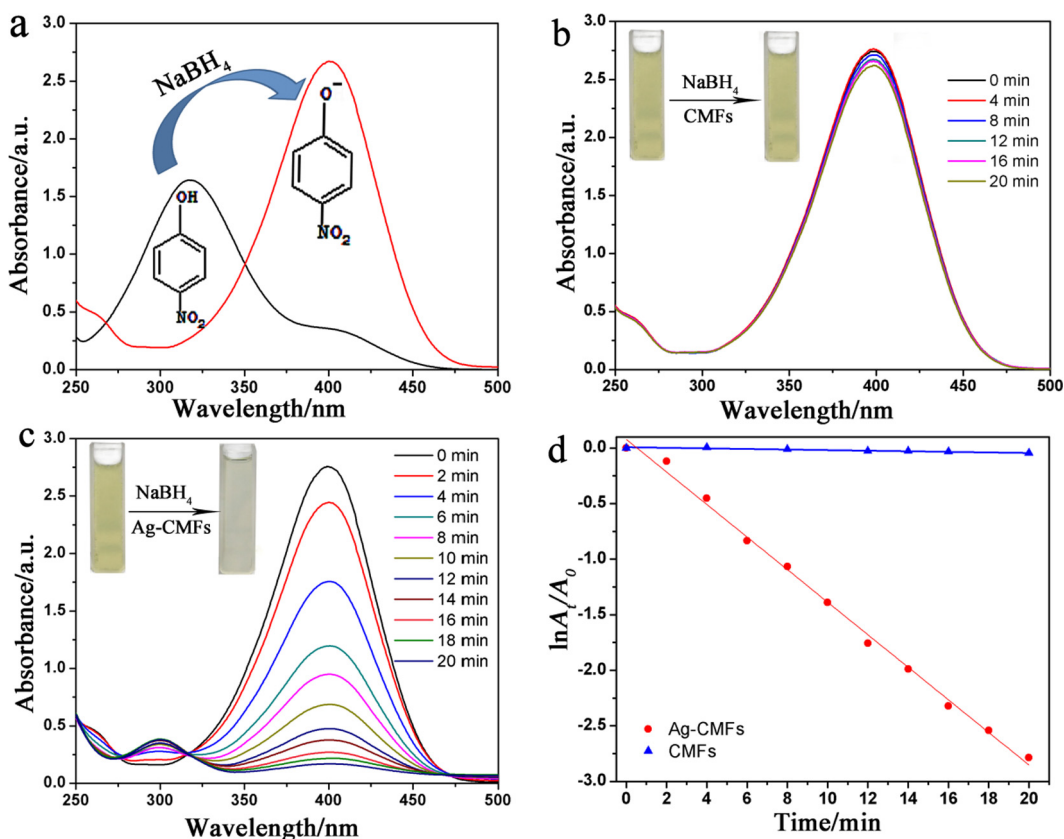


Fig. 5. UV-vis spectra of 4-NP before and after adding  $\text{NaBH}_4$  solution (a), the reduction of 4-NP in the presence of CMFs recorded every 4 min (b), and the reduction of 4-NP in the presence of Ag-CMFs recorded every 2 min (c). Plot of  $\ln(A_t/A_0)$  versus reaction time for the reduction of 4-NP with  $\text{NaBH}_4$  over CMFs and Ag-CMFs (d).

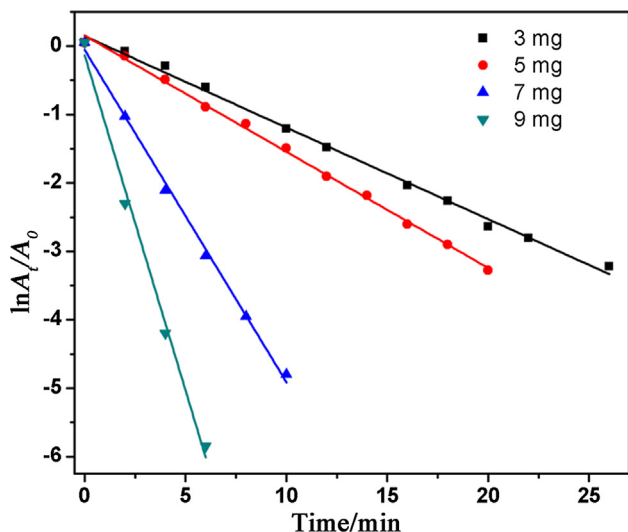


Fig. 6. Plots of  $\ln(A_t/A_0)$  versus reaction time for reduction of 4-NP with  $\text{NaBH}_4$  over different amount of Ag-CMFs.

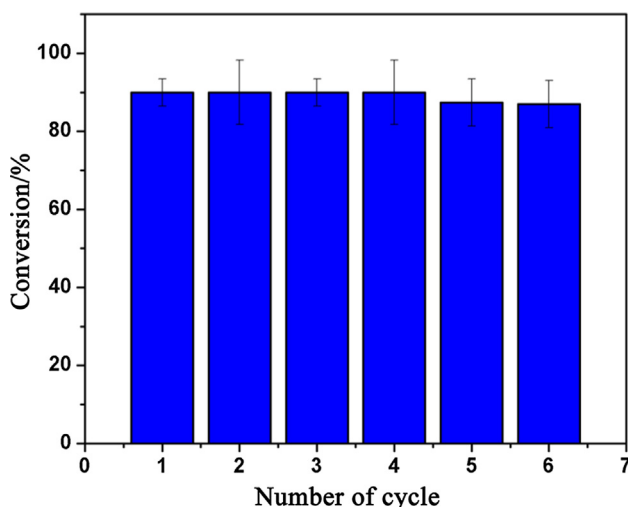


Fig. 7. The reusability of Ag-CMFs as a catalyst for the reduction of 4-NP with  $\text{NaBH}_4$ .

the kinetic rate constant [28,29]. The kinetic equation for the reduction can be written as (Eq. (1)):

$$dC_t/dt = K_{app}C_t \quad \text{or} \quad \ln(C_t/C_0) = \ln(A_t/A_0) = -K_{app}t \quad (1)$$

$C_t$  is the concentration of p-nitrophenol at time  $t$  and  $K_{app}$  is the apparent rate constant, which can be obtained from the decrease of the peak intensity at 400 nm with time. As Fig. 5d shown, linear relationships of  $\ln(A_t/A_0)$  versus reaction time indicate that the reduction of 4-NP employing the Ag-CMFs catalysts well match with pseudo-first-order. The effect of amount of Ag-CMFs on catalytic efficiency as studied as well. As expected, the catalytic efficiency was improved with increasing the amount of catalysts added (Fig. 6). Since the stability of the catalytic activity of heterogeneous catalysts is an important aspect in practical applications, we investigated the reusability of the Ag-CMFs. As shown in Fig. 7, the Ag-CMFs could be conveniently recycled from the reaction solutions and reused for at least six times with a conversion of 87% within 20 min.

#### 4. Conclusion

In summary, we successfully fabricated cellulose-based AgNPs nanocomposites via a wet chemical reduction of AgNPs onto the surface of cellulose microfibrils. Cellulose microfibrils were prepared by deacetylation of electrospun cellulose acetate microfibrils. SEM and TEM indicated the AgNPs decorated on the surface of cellulose microfibrils were very fine and homogeneous. Catalytic activity of the Ag-CMFs was examined by a reduction reaction of 4-NP, the process was recorded by UV-vis spectroscopy, and the catalytic kinetics was also analyzed. It was found that the as-prepared Ag-CMFs nanocomposites exhibit excellent catalytic performance towards the reduction of 4-NP to 4-AP in the presence of  $\text{NaBH}_4$  at room temperature in aqueous media. Moreover, the Ag-CMFs nanocomposites exhibit excellent reusability. The researching work of this paper suggests a new strategy in the design and preparation of silver nanoparticles/cellulose nanocomposite microfibrils, and the products with catalytic property show great promise for the treatment of industrial dye pollutants.

#### Acknowledgements

This investigation was supported by the Jiangsu Province (BK20130969, BK20160017, and BK20160610) and the study was also obtained the partial financial aid from Jiangsu Key Lab of Biomass-based Green Fuels and Chemicals.

#### References

- [1] P.B. Tsekova, M.G. Spasova, N.E. Manolova, N.D. Markova, I.B. Rashkov, Electrospun curcumin-loaded cellulose acetate/polyvinylpyrrolidone fibrous materials with complex architecture and antibacterial activity, *Mater. Sci. Eng. C, Mater. Biol. Appl.* 73 (2017) 206–214.
- [2] M. He, B. Zhang, Y. Dou, G. Yin, Y. Cui, X. Chen, Fabrication and characterization of electrospun feather keratin/poly(vinyl alcohol) composite nanofibers, *RSC Adv.* 7 (16) (2017) 9854–9861.
- [3] A.R. Unnithan, G. Gnanasekaran, Y. Sathishkumar, Y.S. Lee, C.S. Kim, Electrospun antibacterial polyurethane-cellulose acetate-zein composite mats for wound dressing, *Carbohydr. Polym.* 102 (2014) 884–892.
- [4] Y. Wang, H. Huang, G. Li, X. Zhao, L. Yu, C. Zou, Y. Xu, Electrospun TiO<sub>2</sub>-SiO<sub>2</sub> fibres with hierarchical pores from phase separation, *CrystEngComm* 19 (19) (2017) 2673–2680.
- [5] S. Wen, M. Liang, R. Zou, Z. Wang, D. Yue, L. Liu, Electrospinning of palladium/silica nanofibers for catalyst applications, *RSC Adv.* 5 (52) (2015) 41513–41519.
- [6] M. Nasr, R. Viter, C. Eid, R. Habchi, P. Miele, M. Bechelany, Enhanced photocatalytic performance of novel electrospun BN/TiO<sub>2</sub> composite nanofibers, *New J. Chem.* 41 (1) (2017) 81–89.
- [7] O. Arslan, Z. Aytac, T. Uyar, Superhydrophobic, hybrid, electrospun cellulose acetate nanofibrous mats for oil/water separation by tailored surface modification, *ACS Appl. Mater. Interfaces* 8 (30) (2016) 19747–19754.
- [8] L.A. Goetz, B. Jalvo, R. Rosal, A.P. Mathew, Superhydrophilic anti-fouling electrospun cellulose acetate membranes coated with chitin nanocrystals for water filtration, *J. Membr. Sci.* 510 (2016) 238–248.
- [9] K.A. Rieger, H.J. Cho, H.F. Yeung, W. Fan, J.D. Schiffman, Antimicrobial activity of silver ions released from zeolites immobilized on cellulose nanofiber mats, *ACS Appl. Mater. Interfaces* 8 (5) (2016) 3032–3040.
- [10] W. Yang, A.M. Sousa, X. Fan, T. Jin, X. Li, P.M. Tomasula, L. Liu, Electrospun ultra-fine cellulose acetate fibrous mats containing tannic acid-Fe<sup>3+</sup> complexes, *Carbohydr. Polym.* 157 (2017) 1173–1179.
- [11] S. Kota, P. Dumpala, R.K. Anantha, M.K. Verma, S. Kandepu, Evaluation of therapeutic potential of the silver/silver chloride nanoparticles synthesized with the aqueous leaf extract of *Rumex acetosa*, *Sci. Rep.* 7 (1) (2017).
- [12] N.E.-A. El-Naggar, M.H. Hussein, A.A. El-Sawah, Bio-fabrication of silver nanoparticles by phycocyanin, characterization, in vitro anticancer activity against breast cancer cell line and in vivo cytotoxicity, *Sci. Rep.* 7 (1) (2017).
- [13] H. Zheng, D. Ni, Z. Yu, P. Liang, Preparation of SERS-active substrates based on graphene oxide/silver nanocomposites for rapid detection of L-Theanine, *Food Chem.* 217 (2017) 511–516.
- [14] M. Zhang, X. Zhao, G. Zhang, G. Wei, Z. Su, Electrospinning design of functional nanostructures for biosensor applications, *J. Mater. Chem. B* 5 (9) (2017) 1699–1711.
- [15] H. Ma, C. Burger, B.S. Hsiao, B. Chu, Ultra-fine cellulose nanofibers: new nanoscale materials for water purification, *J. Mater. Chem.* 21 (21) (2011) 7507.
- [16] Y. Ahn, D.-H. Hu, J.H. Hong, S.H. Lee, H.J. Kim, H. Kim, Effect of co-solvent on the spinnability and properties of electrospun cellulose nanofiber, *Carbohydr. Polym.* 89 (2) (2012) 340–345.

- [17] K.H. Jang, Y.O. Kang, T.S. Lee, W.H. Park, Photocatalytic activities of cellulose-based nanofibers with different silver phases: Silver ions and nanoparticles, *Carbohydr. Polym.* 102 (2014) 956–961.
- [18] J. Quiros, S. Gonzalo, B. Jalvo, K. Boltes, J.A. Perdigon-Melon, R. Rosal, Electrospun cellulose acetate composites containing supported metal nanoparticles for antifungal membranes, *Sci. Total Environ.* 563–564 (2016) 912–920.
- [19] T. Kamal, I. Ahmad, S.B. Khan, A.M. Asiri, Synthesis and catalytic properties of silver nanoparticles supported on porous cellulose acetate sheets and wet-spun fibers, *Carbohydr. Polym.* 157 (2017) 294–302.
- [20] M. Gopiraman, A.W. Jatoi, S. Hiromichi, K. Yamaguchi, H.Y. Jeon, I.M. Chung, K. Ick Soo, Silver coated anionic cellulose nanofiber composites for an efficient antimicrobial activity, *Carbohydr. Polym.* 149 (2016) 51–59.
- [21] M. Gopiraman, D. Deng, S. Saravananmoorthy, I.-M. Chung, I.S. Kim, Gold, silver and nickel nanoparticle anchored cellulose nanofiber composites as highly active catalysts for the rapid and selective reduction of nitrophenols in water, *RSC Adv.* 8 (6) (2018) 3014–3023.
- [22] W. Li, T. Li, G. Li, L. An, F. Li, Z. Zhang, Electrospun  $H_4SiW_{12}O_{40}$ /cellulose acetate composite nanofibrous membrane for photocatalytic degradation of tetracycline and methyl orange with different mechanism, *Carbohydr. Polym.* 168 (2017) 153–162.
- [23] J.G. Kim, M.C. Cha, J. Lee, T. Choi, J.Y. Chang, Preparation of a sulfur-functionalized microporous polymer sponge and in situ growth of silver nanoparticles: a compressible monolithic catalyst, *ACS Appl. Mater. Interfaces* (2017).
- [24] F. Hamano, H. Seki, M. Ke, M. Gopiraman, C.T. Lim, I.S. Kim, Cellulose acetate nanofiber mat with honeycomb-like surface structure, *Mater. Lett.* 169 (2016) 33–36.
- [25] M. Gopiraman, H. Bang, G. Yuan, C. Yin, K.H. Song, J.S. Lee, I.M. Chung, R. Karvembu, I.S. Kim, Noble metal/functionalized cellulose nanofiber composites for catalytic applications, *Carbohydr. Polym.* 132 (2015) 554–564.
- [26] Z. Wu, X. Mao, Q. Zi, R. Zhang, T. Dou, A.C.K. Yip, Mechanism and kinetics of sodium borohydride hydrolysis over crystalline nickel and nickel boride and amorphous nickel–boron nanoparticles, *J. Power Sources* 268 (2014) 596–603.
- [27] W. Zhang, Y. Sun, L. Zhang, Fabrication of high efficient silver nanoparticle catalyst supported on poly(glycidyl methacrylate)–polyacrylamide, *Ind. Eng. Chem. Res.* 55 (48) (2016) 12398–12406.
- [28] H. Mao, C. Ji, M. Liu, Z. Cao, D. Sun, Z. Xing, X. Chen, Y. Zhang, X.-M. Song, Enhanced catalytic activity of Ag nanoparticles supported on polyacrylamide/polypyrrole/graphene oxide nanosheets for the reduction of 4-nitrophenol, *Appl. Surf. Sci.* 434 (2018) 522–533.
- [29] P. Sudhakar, H. Soni, Catalytic reduction of Nitrophenols using silver nanoparticles-supported activated carbon derived from agro-waste, *J. Environ. Chem. Eng.* 6 (1) (2018) 28–36.